

Physiochemical and Electrochemical Properties of Lanthanum Strontium Cobalt Ferum–Copper (II) Oxide Prepared via Solid State Reaction

Ahmad Fuzamy Mohd Abdul Fatah, Muhamad Nazri Murat and NoorAshrina A. Hamid*

School of Chemical Engineering, Engineering Campus, Universiti Sains Malaysia,
14300 Nibong Tebal, Malaysia

* Corresponding author: chrina@usm.my

Published online: 30 November 2022

To cite this article: Ahmad Fuzamy, M. A. F. et al. (2022). Physiochemical and electrochemical properties of lanthanum strontium cobalt ferum–copper (II) oxide prepared via solid state reaction. *J. Phys. Sci.*, 33(3),101–117. <https://doi.org/10.21315/jps2022.33.3.7>

To link to this article: <https://doi.org/10.21315/jps2022.33.3.7>

ABSTRACT: *Lanthanum strontium cobalt ferum (LSCF) with addition of copper oxide (CuO) can serve as an alternate cathode material in Intermediate Temperature Solid Oxide Fuel Cell (IT-SOFC) due to its strong catalytic activity for oxygen reduction process at intermediate temperatures and great chemical compatibility. This study was done to determine the viability of LSCF–CuO composite as a material for the IT-SOFC cathode. The cathode powder was synthesised using the conventional solid-state process at intermediate temperatures range (600°C–900°C). The thermogravimetric analysis demonstrated that when LSCF was calcined at temperatures over 600°C, the weight loss curve flattened. In the meantime, x-ray diffraction revealed that the perovskite structure of LSCF–CuO was completely formed after calcined at 800°C. Moreover, the Brunauer–Emmett–Teller (BET) and scanning electron microscope investigations demonstrated that as the calcination temperature rose, the LSCF–CuO particles tended to grow. The electrochemical impedance spectroscopy investigation revealed polarisation resistance of samples calcined at 800°C (0.41 Ωcm^2) was significantly lower than that of samples calcined at 600°C (29.57 Ωcm^2). Judging from chemical, physical and electrochemical properties, it is evidence that LSCF–CuO prepared via simple solid-state reaction has a potential to be used as cathode material for IT-SOFC.*

Keywords: LSCF–CuO cathode, intermediate temperature solid oxide fuel cell, perovskite, solid-state method

1. INTRODUCTION

The solid-state synthesis approach necessitates high temperatures to synthesise micro to nanoscale solid materials. It is the favoured method of synthesis due to its simplicity and little solvent usage. It is very important that the materials used in the cathode are free of contaminants and can make nano-sized particles. This procedure also involves milling, which is employed to minimise the particle size of the resulting nanomaterials.¹ The cathode can be made even more compact by reducing the particle size. In this way, the degradation rate is expected to be reduced.

Initial phases of the typical solid-state process involve mixing and grinding. Mixing raw materials with ethanol and milling them for a particular amount of time. Using ethanol prevents raw materials from adhering to a grinding surface.^{2,3} Because ethanol may be easily removed at its boiling point of roughly 80°C, it necessitates greater care during milling.² The resulting mixture is dried in an oven to eliminate surplus ethanol and nitrate from the metal nitrate. Several modified solid-state routes necessitate both the vaporisation and grinding procedures. Individually preheating all input materials to eliminate nitrate is the first step of the solid-state reaction (SSR) technique. Then, the basic components are combined in the required proportions. The resulting metal oxide is subsequently milled to reduce its particle size. The purpose of employing metal oxide as a material prior to a mixing operation is to guarantee that nitrate is eliminated prior to the beginning of synthesis.^{4,5} The mixture is heated to eliminate ethanol and the resulting powder is next crushed and sifted to avoid the incorporation of big particles.

To increase the efficiency of a solid oxide fuel cell (SOFC), noble metals can be added to the cathode using the composite cathode technique. The difficulties of matching mixed ionic–electronics cathode (MIEC) materials with another noble metal can make the implementation of composite cathodes complicated.⁶ Since each material has its own restrictions, it is challenging to establish the ideal operating conditions. The primary objective of using composite cathodes is to increase electrocatalytic activity. According to several studies, addition of copper oxide (CuO) composite with various combination of electrolytes and cathodes can provide excellent sintering aids and catalytic reactions for ceramics.^{7–9} CuO infiltration is a cost-effective and efficient approach for increasing the catalytic stability of cathodes.^{10,11} Consequently, it is vital to comprehend the mechanisms underlying the observed improvement in the oxygen reduction reaction's (ORR) production and effective stability.

Adoption of $\text{La}_{0.6}\text{Sr}_{0.4}\text{Co}_{0.2}\text{Fe}_{0.8}\text{O}_3$ (LSCF) as the cathode MIEC material in SOFC is a popular topic of discussion in contemporary fuel cell research. Through oxide materials, lattice oxide are carrying the oxygen ions, which is classified as a perovskite structure of the LSCF, with lanthanum oxide and strontium oxide occupying the A-site and cobalt oxide and ferrite oxide occupying the B-site.¹² When the A-site cations are the same size as the oxygen ions, the cubic close-packed structure is attained. The B-site cations would occupy exclusively oxygen-atom-formed octahedral holes which would be perfect orthorhombic.¹³ The inclusion of transition metal ($\text{Cu} = 0.74 \text{ \AA}$) affects the B-site by substituting the oxygen ion with the appropriate transition metal ion. This alters the lattice parameters that characterise the oxygen vacancy intensity in the composites' cathode. As a result, this work concentrated on fabricating the LSCF–CuO cathode for IT-SOFC using the usual solid-state approach and determining its physical, chemical and electrical properties.

2. METHODOLOGY

The starting materials for the sol–gel synthesis of LSCF were lanthanum nitrate hexahydrate ($\text{La}(\text{NO}_3)_3 \cdot 6\text{H}_2\text{O}$, MERCK Sdn Bhd., Malaysia), strontium nitrate hexahydrate ($\text{Sr}(\text{NO}_3)_2$, Friendemann Schmidt Chemicals, Germany), cobalt nitrate hexahydrate ($\text{Co}(\text{NO}_3)_2 \cdot 6\text{H}_2\text{O}$, ChemAR®, Malaysia), ferrite nitrate nonahydrate ($\text{Fe}(\text{NO}_3)_3 \cdot 9\text{H}_2\text{O}$, ChemPur®, Malaysia). The chemicals used in the symmetric cell processing were ethylenediaminetetraacetic acid ($\text{C}_4\text{H}_8\text{N}_2\text{O}_8$, Sigma-Aldrich®, Malaysia), terpineol ($\text{C}_{10}\text{H}_{18}\text{O}$, Sigma-Aldrich®, Malaysia), ethyl cellulose ($\text{C}_{23}\text{H}_{24}\text{N}_6\text{O}_4$, Sigma-Aldrich®, Malaysia), copper nitrate ($\text{Cu}(\text{NO}_3)_2 \cdot 3\text{H}_2\text{O}$, Sigma-Aldrich®, Malaysia).

For this experiment, 6:4:2:8 ratios of the metals La, Sr, Co and Fe were used to mixed with excess ethyl alcohol in beakers. This mixture was then transferred to a beaker and agitated until a homogenous mixture was created. The resulting solution was calcined at various temperatures (600°C – 800°C) to create LSCF powder. Physical mixing by pestle and mortar is recognised for combination of ceramic material. In this work, LSCF and CuO powder was amalgamated at weight ratio 95:5 using pestle and mortar followed by calcination process at 800°C to create LSCF–CuO composite powder. It is proven that resultant mixture of LSCF–CuO prepared via pestle and mortar is homogenous as reported by previous work.¹⁴

The cathode ink was produced by mixing at ratio of 7:13 vehicle ink and LSCF–CuO. Samarium-doped ceria ($\text{Sm}_{0.2}\text{C}_{0.8}$) material was compressed to 13 mm pellets at 250 Mpa and sintered at 1300°C for 6 h. LSCF–CuO ink was painted on both sides of the Samarium Doped Ceria (SDC) electrolyte via painting brush (Faber

Castle®, type nylon) to produce a symmetric cell. The coated SDC electrolyte were then sintered at 1100°C to eliminate excess binder. The LSCF–CuO surface was entirely covered with thin platinum paste to function as the current collector layer.

The precursor powder's thermal breakdown behaviour was examined using a thermogravimetric analyser (TGA, model PerkinElmer STA 600, USA) at air flow rate of 50 cm³/min and a heating rate of 5°C/min and from 30°C to 900°C. Bruker AXS GmbH X-ray, Germany diffraction (XRD) was used to determine the phase composition of the pellet ranging from 10° to 90°, with Cu–K radiation. Using the X'Pert HighScore Plus program, the data from the XRD analysis were evaluated. The primary sample of LSCF–CuO at 800°C was compared to data from the literature and samples of synthesised LSCF and CuO. Crystallite size of LSCF and CuO was calculated via Scherrer equation as depicted in the following equation.¹⁵

$$D = 0.9\lambda/(\beta\cos\theta)$$

Where,

D = Crystallite size

λ = X-ray wavelength (CuK α = 0.154)

β = line broadening at half the maximum intensity (FWHM)

θ = Bragg angle

Perovskite percentage was calculated via swart and shroud equation as in the following equation.¹⁶

$$\text{Perovskite phase (wt\%)} = \frac{I_p}{I_p - I_m} \times 100\%$$

Where,

I_p = peak intensity of the preferred perovskite

I_m = peak intensity of the unwanted phase

A Quanta FEG 650, USA was employed to examine the LSCF–CuO powder's microstructure. Using a backscattered electron, the acceleration voltage applied was 5 kV–15 kV. Meanwhile, the microstructural behaviour of the sample was determined at 500 nm and 5 μ m. Total pore volume and specific surface area of

the LSCF–CuO sample were determined using Brunauer–Emmett–Teller (BET) Micromeritics ASAP 2020, USA with an average sample mass of 0.2 g.

Electrochemical impedance spectroscopy (EIS) with a furnace setup was utilised to evaluate the electrode-solution interactions (model ZIVE SP2, South Korea). For this investigation, an SDC cell of 11 mm in diameter was employed as the electrolyte, and the LSCF–CuO cathode was placed on both sides of the pellet to create symmetric cells. The surface of the electrodes, which had been covered with platinum paste, was adorned with silver wires. Each sample was measured at a temperature between 600°C and 800°C with a frequency range of 0.1 Hz to 1 MHz and a signal amplitude of 10 mV. Using a type-K thermocouple, the polarisation cell was measured on a Digi-Sense digital thermocouple thermometer (Eutech Instrument). The ZMAN 2.4 (ZIVE LAB) software was used to analyse raw data and convert them to the equivalent circuits, and the SigmaPlot software version 11 was used to visualise each of them. This examination was conducted in the open air.

3. RESULTS AND DISCUSSION

As shown in Figure 1, thermogravimetric analysis can represent weight loss vs the temperature. The graph depicts three segments of weight loss that occur at varying temperatures. The elimination of adsorbed water, nitrate degradation and ethanol removal happened between 30°C and 400°C. This could be since water has a boiling point of 100°C, whereas nitrates often break down at temperatures above 200°C. This conclusion is supported by differential thermal gravimetry (DTG), which revealed a significant peak emerging at 150°C, indicating the total removal of water from the solution, and a shorter peak emerging at 80°C, showing the entire removal of nitrate from the solution.

In the second phase, the slope of weight loss between 400°C and 600°C was less steep. Decomposition of the metal-citrate complex was also observed, suggesting that metal salts developed a single-phase perovskite. This is a vital phase as the production of LSCF begins with continuous weight loss, which represents the continuing of LSCF formation and the development of oxygen vacancies.^{17–19} The DTG peak at 580°C suggested the contraction of metal ions and the production of lattice oxygen.

The third phase exhibited a slight weight loss which represents LSCF perovskite stabilisation and formation of oxygen vacancies occurrence. Several studies who previously explored the effects of TGA on MIEC have highlighted this result.^{18,20,21} The results also indicated that the initial elimination stage (30°C–400°C) causes a

significant weight loss. It might be described further that the first stage contained organic components such as water, nitrate and ethanol, which combined in the initial phase and were removed based on their boiling points (water, 100°C; nitrate in metal salt, 70°C; and ethanol, 78°C). It was determined that phase purity contributed to the enhancement of oxygen vacancy formation. Thus, it may be explained that as oxygen vacancies rise, so do pores and active surface area. Therefore, more ORR is created, leading to an increase in electrical conductivity.¹⁸

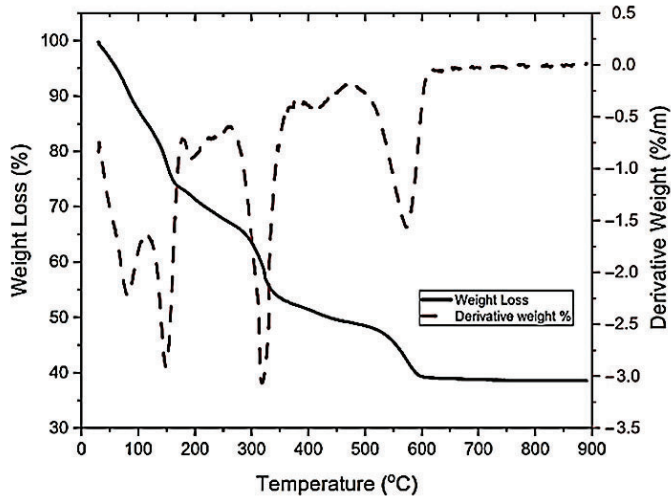


Figure 1: TGA/differential thermal analysis (DTA) analysis of LSCF synthesised using the solid-state method at precursor state.

Crystallinity and purity of composite LSCF–CuO was determined using XRD as illustrated by Figure 2. LSCF–CuO XRD data were compared to LSCF and CuO XRD data. LSCF was matched with JCPDS 01-089-1268 and CuO JCPDS 01-080-1917. As some undefined peaks were seen between 10° and 30° at temperatures below 800°C, the XRD analysis revealed that all LSCF–CuO powder samples formed entirely at temperatures above 800°C. The unexplained peak at 15° for LSCF–CuO calcined at 600°C suggested that LSCF perovskite production was incomplete. Further research utilising X’Pert HighScore Plus indicated that the peak in the A-site area belonged to La_2O_3 and SrCO_2 , in accordance with other previous articles.^{14,22,23} Although the thermal analysis previously suggested that the weight loss after calcining at 600°C is flattened, phase analysis confirmed LSCF that was calcined at 800°C produce a complete perovskite structure among candidates.

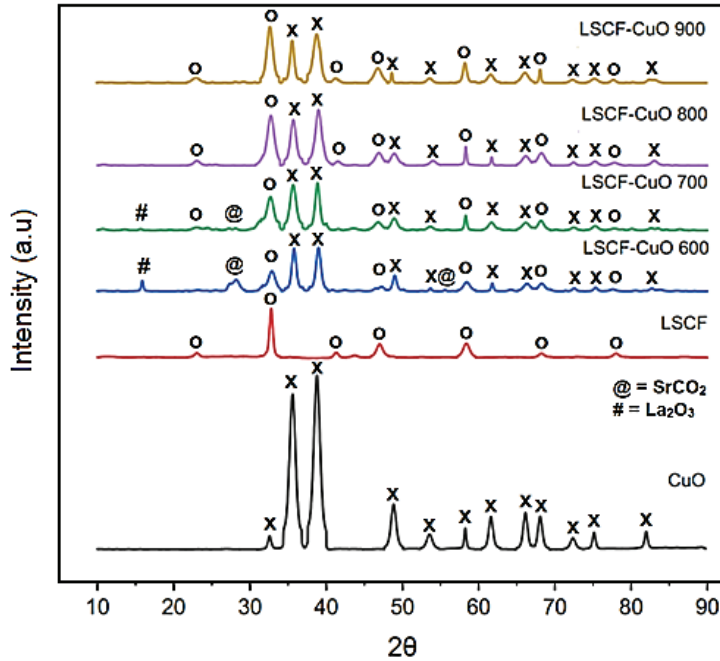


Figure 2: XRD analysis of LSCF–CuO at different calcination temperatures (600°C–900°C)

The Swarts and ShROUT equation was used to calculate the percentage of perovskite phase, which is detailed in Table 1.²⁴ The maximum intensity was derived from the highest peak intensity of LSCF, but the impurity peak could only be determined by setting the minimum peak intensity to 35.72 a.u. After being calcined at 800°C, it was confirmed that LSCF achieves a full perovskite structure, since the obtained perovskite phase percentage for each sample is greater than 90%. If the perovskite percentage is greater than 90%, the perovskite structure will retain its behaviour.^{25,26}

Table 1: Perovskite percentage of LSCF–CuO by varies calcination temperature.

Sample (LSCF–CuO)	Crystalline Phase	Percentage of perovskite phase LSCF (%)
Solid State 600°C	LSCF, CuO	79.218
Solid State 700°C	LSCF, CuO	83.162
Solid State 800°C	LSCF, CuO	96.798
Solid State 900°C	LSCF, CuO	97.941

Bragg's method was applied to the XRD data to verify the perovskite structure of LSCF–CuO calcined at 800 °C. In-depth calculations were reported in Table 2, and it was demonstrated that all peak errors were less than 1%.²⁷ It was confirmed that LSCF calcined at 800 °C possessed an orthorhombic structure while CuO having a monoclinic structure. It also demonstrated that the inclusion of metal oxide candidates is conceivable due to the vast differences in cell volume.²⁸ Consequently, CuO able to bridge the LSCF particle gap. Therefore, the ideal LSCF–CuO calcination temperature was selected to 800 °C because neither an additional nor a shifted peak was noticed. This revealed that the penetration of CuO into the B-site of LSCF is plausible, given that the two chemicals are chemically compatible.

Table 2: Lattice constant of LSCF–CuO (JCPDS card LSCF: 01-089-1268, CuO: 01-080-1917).

Sample	Element	Structure	Lattice constant (Å)			Volume of cell (10 ⁶ pm ³)
			a	b	c	
LSCF–CuO	LSCF	Orthorhombic	5.470	5.486	7.854	235.686
	CuO	Monoclinic	4.648	3.631	5.103	86.123

Analyses of surface area were performed to determine the specific surface area of LSCF–CuO powder with varying calcination temperatures. Table 3 displays the specific surface area derived from BET analysis, the mean particle size derived from scanning electron microscopy (SEM) analysis, and the crystallite size estimated using the Scherrer equation and XRD data. The table shows that surface area decreases with rising temperature. The main factor contributing on decreasing specific surface area is increasing of calcination temperature is increase in grain size and larger granulation which subsequently increasing the overall particle size.^{14,29–31} This pattern is consistent with the mean particle size determined by SEM and the crystallite size calculated by XRD. As a result, LSCF–CuO calcined at 800 °C was chosen as a candidate for symmetric cell processing due to its nanoparticle size (< 100nm).

Table 3: BET analysis and crystallite size of LSCF–CuO at the respective calcination temperature.

Sample (LSCF–CuO)	Specific surface area (m ² /g)	Mean particle size (nm)	Crystallite size (nm)
Solid State 600°C	13.33	70.113	14.39
Solid State 700°C	10.55	75.442	14.62
Solid State 800°C	7.02	84.355	16.17
Solid State 900°C	4.47	122.641	32.34

The electrochemical performance of the symmetric cathode was evaluated, and the cathode sintered at 800°C was chosen for EIS testing based on the BET analysis. Figure 3 illustrates the selection of the equivalent circuit for the complete sample. L_s , R_s , R_1 , and Q_1 indicated the EIS silver current–voltage probes' inductance based on the ZMAN software's equivalent circuit and fitting parameters. R_s was classified as R_{ohm} , denoting the silver wire and the electrolyte resistance. R_1 and Q_1 indicate low-frequency arcs, with R representing the polarisation resistance at respective arc and Q representing the constant phase element.

It is prudent to first assess the activation energy required to construct LSCF–CuO symmetric cells, as the activation energy reflects the cell's overall performance as the operating temperature varies.³² The activation energy computed from the polarisation resistance is as low as 166 kJ/mol, as seen in Figure 3(a). This finding was significantly lower than the commercial LSCF measurement of 186 kJ/mol.³⁰ The fact that LSCF–CuO has a lower activation energy than commercial LSCF demonstrated that CuO capable to function as a synergistic catalyst.^{6,33}

Based on Figure 3(b), this finding may be explained by the fact that the LSCF–CuO cathode has a stable energy at a high working temperature of 800°C to accomplish side-to-side ion exchange. The results demonstrate that LSCF–CuO 800°C is an appropriate cathode choice for IT-SOFCs, as previous research indicates that a good cathode must have a resistance of less than 1 Ωcm^{-2} .³⁴

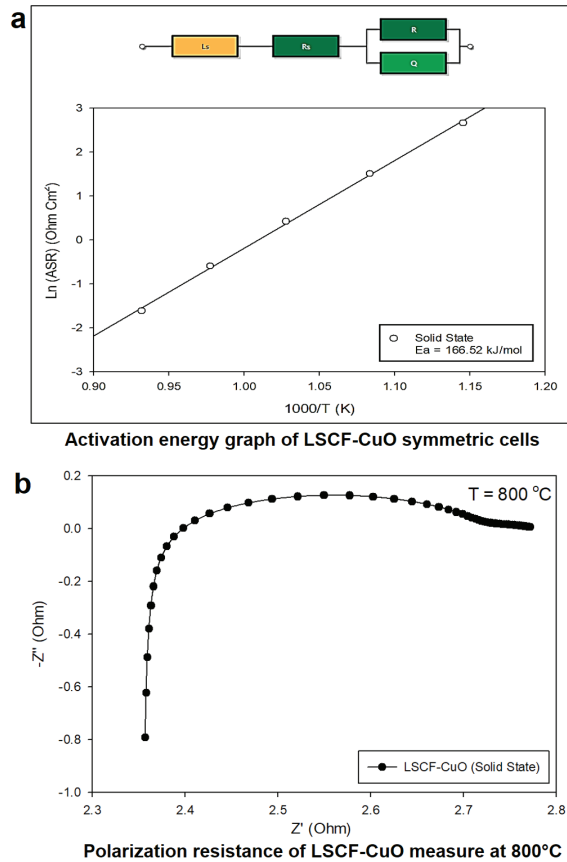


Figure 3: (a) Corresponding circuit and activation energy of the LSCF-CuO symmetric cell and (b) polarisation resistance of LSCF-CuO operated at 800°C.

The focus of further investigation is the area specific resistance (ASR) of an LSCF-CuO symmetric cell operating between 800°C and 600°C. Figure 4(a) demonstrates that the overall ASR of LSCF-CuO grows progressively as the operating temperature decreases. This result also demonstrated that CuO was successfully infused into the B-site of the LSCF cathode. However, polarisation resistance was greater at 600°C than 800°C. This could be since the ORR at 600°C was lower than that at 800°C due to the progressive increase in polarisation resistance cause by inability of ions to flow through the electrolyte resistance.

As shown in Figure 4(b), thermal study was performed on LSCF-CuO powder calcined at 800°C for 6 h to support the EIS conclusion on the effect of operating temperature. Starting from room temperature up to 300°C, the graph for weight

loss indicates a significant weight loss, which can be explained by the elimination of absorbed water and other contaminants. Based on the thermal graph, the weight loss of LSCF–CuO decreases continuously from 600°C to 800°C, showing that 800°C produces the most oxygen lattice. In SOFC cells, the oxygen lattice contributes to the ORR which increased lattice oxygen results in a higher electron transport path.³⁵ In comparison to 600°C operating temperature, 800°C operating temperature produces the lowest polarisation resistance.

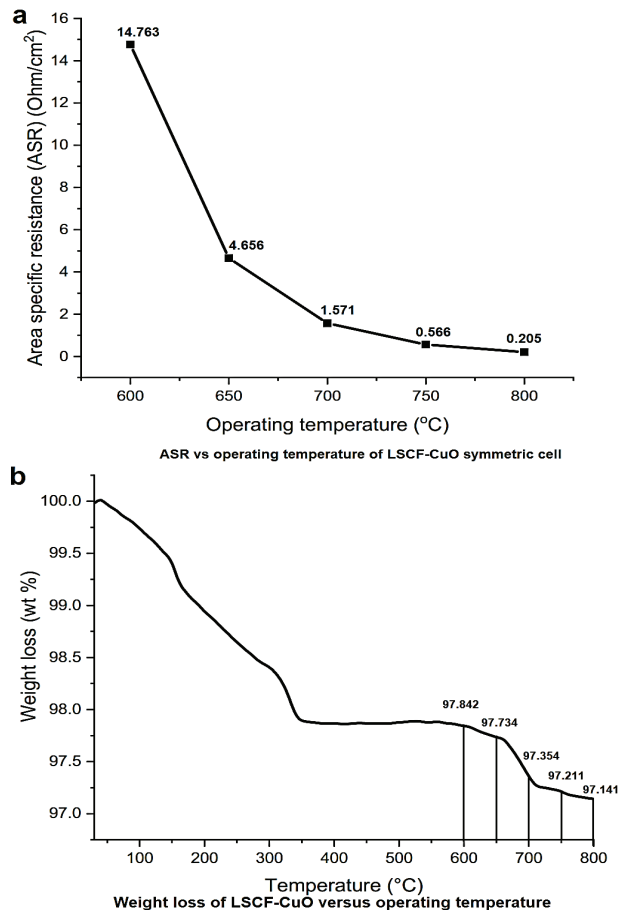


Figure 4: (a) Area specific resistance (ASR) versus operating temperature of LSCF–CuO symmetric cell fabricated via LSCF–CuO powder that was calcined at 800°C and (b) Weight loss of LSCF–CuO powder that was calcined at 800°C versus temperature.

Post-characterisation was performed on the symmetric cell surface of LSCF–CuO. As shown in Figure 5(a), the samples were further analysed by SEM to explore the morphology of the LSCF–CuO composite. The LSCF–CuO surface is predominantly porous. This cathode was used to make well-structured porosity because the orthorhombic structure could form a sharp edge that made a space between each other.³⁶ These small granules were densely interconnected.

In general, a rise in sintering temperature results in an increase in grain size and a subsequent diminution of the surface area–gas solid interface (triple boundary phase).²¹ Our condition increased the polarisation resistance in this investigation. During EIS characterisation, however, an increase in sintering temperature could cause the electrode particles to aggressively attach to the electrolyte surface.³⁷ In conclusion, calcining LSCF–CuO powder at 800°C and sintering LSCF–CuO symmetric cell at 1100°C is an appropriate temperature for the LSCF–CuO fabrication process.

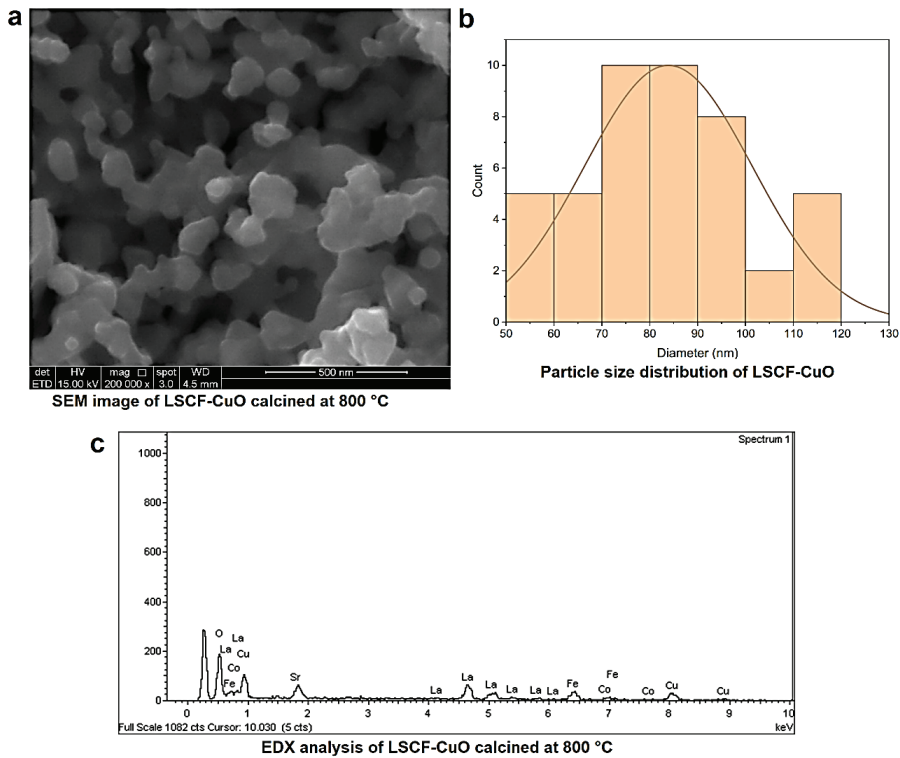


Figure 5: (a) SEM image of LSCF–CuO that was calcined at 800°C microstructure, (b) particle size distribution of LSCF–CuO that was calcined at 800°C from image and (c) EDX analysis of LSCF–CuO that was calcined at 800°C.

Further investigation was conducted using the LSCF–CuO samples at different calcination temperatures via the energy dispersive x-ray (EDX) analysis. As shown in Figure 5(b), the results indicate that the synthesised LSCF–CuO samples are pure at all calcination temperatures. The peaks have been identified as lanthanum, strontium, cobalt, ferrite, copper and oxygen based on the graph. As no contaminants were discovered in the samples, this result indicated that the resulted pure LSCF–CuO powder was obtained. Several similarities were noticed between all the EDX graphs, in which LSCF elements were observed to have a low electric value and a similar trend of location.

CuO was discovered as a trace during EDX analysis, where it improved the conductivity of the samples. Oxygen's spectrum has the largest peak, followed by lanthanum and strontium, among other elements, as determined by more research. This is due to the extremely high ionic radii of oxygen, lanthanum and strontium.³⁸ Consequently, these peaks will be superior to those of other elements since they are clearly detectable.¹² EDX examination revealed no evidence of SDC electrolyte, indicating that no active chemical reaction occurred between LSCF–CuO and SDC during operation.

4. CONCLUSION

In conclusion, LSCF–CuO indeed capable to act as cathode material for solid oxide fuel cell (IT-SOFCs) that operate at 800°C. Although thermal analysis showed precursor LSCF attained zero loss of weight after calcined 600°C, thermal analysis revealed that several peaks known as SrCO₂ and LaCO₃ presented as LSCF–CuO that was calcined at 600°C and 700°C. The presence of SrCO₂ and LaCO₃ was completely removed after the sample were calcined above 800°C. On top of that, LSCF–CuO that was calcined at 800°C and 900°C also showed high perovskite percentage which is 96.79% and 97.94%. In conjunction with phase and thermal analysis, surface morphology analysis revealed that increasing calcination temperature of LSCF–CuO powder led to an increase in particle size and a decrease in the triple phase boundary. However, LSCF–CuO that was calcined at 800°C capable to attain average nanoparticle size which is 84.35 nm. Therefore, as LSCF–CuO that was calcined at 900°C produce 122.64 nm which is offside from nano size range (< 100 nm), LSCF–CuO calcined at 800°C was chosen as subject for EIS analysis. In accordance with results of the characterisation, LSCF–CuO that was calcined at 800°C was chosen for the EIS analysis. The area specific resistance of a symmetric LSCF–CuO cell was as low as 0.205 Ω cm⁻² at an operating temperature of 800°C and an activation energy of 166.52 kJ/mol. Based on the physical, chemical and electrochemical analysis of LSCF–CuO

examined in this work, this shows that it is possible for LSCF–CuO to act as cathode candidate for intermediate temperature SOFCs.

5. ACKNOWLEDGEMENTS

This research was fully funded by the Ministry of Science, Technology & Innovation (MOSTI) under the Fundamental Research Grant Scheme (FRGS/203/PJKIMIA/6071343). The authors are grateful to Associate Prof. Dr Nafisah Osman for her insight into EIS measurements that were conducted in her laboratory.

6. REFERENCES

1. Niemczyk, A. et al. (2018). Assessment of layered $\text{La}_{2-x}(\text{Sr},\text{Ba})_x\text{CuO}_{4-\delta}$ oxides as potential cathode materials for SOFCs. *Int. J. Hydrog. Energy*, 43(32), 15492–15504. <https://doi.org/10.1016/j.ijhydene.2018.06.119>
2. Zhou, Q. et al. (2015). Synthesis and characterization of $\text{BaBi}_{0.05}\text{Co}_{0.8}\text{Nb}_{0.15}\text{O}_{3-\delta}$ as a potential IT-SOFCs cathode material. *J. Alloys Compds*, 627, 320–323. <https://doi.org/10.1016/j.jallcom.2014.11.187>
3. Mao, X. et al. (2015). A novel cobalt-free double-perovskite $\text{NdBaFe}_{1.9}\text{Nb}_{0.1}\text{O}_{5+\delta}$ cathode material for proton-conducting IT-SOFC. *Ceram. Int.*, 41(8), 10276–10280. <https://doi.org/10.1016/j.ceramint.2015.03.326>
4. Da Rosa Silva, E. et al. (2019). The effect of calcination atmosphere on structural properties of Y-doped SrTiO_3 perovskite anode for SOFC prepared by solid-state reaction. *Ceram. Int.*, 45(8) 9761–9770. <https://doi.org/10.1016/j.ceramint.2019.02.011>
5. Tyagi, D. et al. (2018). XPS studies of Sr doped La_2CuO_4 : A potential cathode material for IT-SOFCs. *Mater.*, 5(11), 22950–22954. <https://doi.org/10.1016/j.matpr.2018.11.022>
6. Gao, C. et al. (2017). Improve the catalytic property of $\text{La}_{0.6}\text{Sr}_{0.4}\text{Co}_{0.2}\text{Fe}_{0.8}\text{O}_{3/\text{Ce}_{0.9}\text{Gd}_{0.1}\text{O}_2}$ (LSCF/CGO) cathodes with CuO nanoparticles infiltration. *Electrochim. Acta*, 246, 148–155. <https://doi.org/10.1016/j.electacta.2017.05.138>
7. Baqer, A. A. et al. (2018). Synthesis and characterization of binary $(\text{CuO})_{0.6}(\text{CeO}_2)_{0.4}$ nanoparticles via a simple heat treatment method. *Results Phys.*, 9, 471–478. <https://doi.org/10.1016/j.rinp.2018.02.079>
8. Tian, N. et al. (2020). Properties of $\text{Ce}_{0.85}\text{Sm}_{0.15}\text{O}_{2-\delta}$ -CuO electrolytes for intermediate-temperature solid oxide fuel cells. *Solid State Ion.*, 351, 115331. <https://doi.org/10.1016/j.ssi.2020.115331>
9. Lima, C. G. M., Santos, T. H., Grilo, J. P. F., Dutra, R. P. S., Nascimento, R. M., Rajesh, S., Fonseca, F. C., & Macedo, D. A. (2015). Synthesis and properties of CuO-doped $\text{Ce}_{0.9}\text{Gd}_{0.1}\text{O}_{2-\delta}$ electrolytes for SOFCs. *Ceram. Int.*, 41(3), 4161–4168. <https://doi.org/10.1016/j.ceramint.2014.12.093>

10. Biswas, M. et al. (2016). Low-temperature sintering of Ba(Zr,Y)O₃-based proton conducting oxides using BaO–CuO eutectic flux as sintering aid. *Ceram. Int.*, 42(8), 10476–10481. <https://doi.org/10.1016/j.ceramint.2016.03.038>
11. Shen, Z. et al. (2017). Effect of CuO addition on crystallization and thermal expansion properties of Li₂O–ZnO–SiO₂ glass-ceramics. *Ceram. Int.*, 43(9), 7099–7105. <https://doi.org/10.1016/j.ceramint.2017.02.141>
12. Guo, S. et al. (2015). B-Site metal (Pd, Pt, Ag, Cu, Zn, Ni) promoted La_{1-x}Sr_xCo_{1-y}FeyO_{3-δ} perovskite oxides as cathodes for IT-SOFCs. *Catalysts*, 5(1), 366–391. <https://doi.org/10.3390/catal5010366>
13. Kumar, S. A. et al. (2018). Auto-combustion synthesis and electrochemical studies of La_{0.6}Sr_{0.4}Co_{0.2}Fe_{0.8}O_{3-δ} – Ce_{0.8}Sm_{0.1}Gd_{0.1}O_{1.90} nanocomposite cathode for intermediate temperature solid oxide fuel cells. *Ceram. Int.*, 44(17), 21188–21196. <https://doi.org/10.1016/j.ceramint.2018.08.164>
14. Rosli, A. Z. et al. (2021). Physical characterization of LSCF–NiO as cathode material for intermediate temperature solid oxide fuel cell (IT-SOFCs). *Mater.*, 46(5), 1895–1900. <https://doi.org/10.1016/j.matpr.2021.01.778>
15. Ji, B. et al. (2016). Magnetic properties of samarium and gadolinium co-doping Mn-Zn ferrites obtained by sol-gel auto-combustion method. *J. Rare Earths*, 34(10), 1017–1023. [https://doi.org/10.1016/s1002-0721\(16\)60129-1](https://doi.org/10.1016/s1002-0721(16)60129-1)
16. Osman, N. et al. (2020). Optimization of electrolyte performance by tailoring the structure and morphology of Ba(Ce,Zr)O₃ ceramics with different types of surfactants. *Ceram. Int.*, 46(17), 27401–27409. <https://doi.org/10.1016/j.ceramint.2020.07.226>
17. Costilla-Aguilar, S. U. et al. (2021). Double perovskite La_{1.8}Sr_{0.2}CoFeO_{5+δ} as a cathode material for intermediate temperature solid oxide fuel cells. *J. Alloys Compd.*, 862, 158025. <https://doi.org/10.1016/j.jallcom.2020.158025>
18. Junior, V. P. et al. (2018). Enhanced LSCF oxygen deficiency through hydrothermal synthesis. *Ceram. Int.*, 44(17), 20671–20676. <https://doi.org/10.1016/j.ceramint.2018.08.060>
19. Mani, R. et al. (2015). A Study on La_{0.6}Sr_{0.4}Co_{0.3}Fe_{0.8}O₃(LSCF) cathode material prepared by gel combustion method for IT-SOFCs: Spectroscopic, electrochemical and microstructural analysis. *Asian J. Research Chem.*, 8(6), 389–393. <https://doi.org/10.5958/0974-4150.2015.00062.0>
20. Garcia, L. M. P. et al. (2013). Citrate–hydrothermal synthesis, structure and electrochemical performance of La_{0.6}Sr_{0.4}Co_{0.2}Fe_{0.8}O_{3-δ} cathodes for IT-SOFCs. *Ceram. Int.*, 39(7), 8385–8392. <https://doi.org/10.1016/j.ceramint.2013.04.019>
21. da Conceição, L. et al. (2011). Combustion synthesis of La_{0.7}Sr_{0.3}Co_{0.5}Fe_{0.5}O₃ (LSCF) porous materials for application as cathode in IT-SOFC. *Mat. Res. Bull.*, 46(2), 308–314. <https://doi.org/10.1016/j.materresbull.2010.10.009>
22. Rahayu, S. et al. (2021). Facile Synthesis of Lanthanum Strontium Cobalt Ferrite (LSCF) Nanopowders Employing an Ion-Exchange Promoted Sol-Gel Process. *Energies*, 14(7), 1800. <https://doi.org/10.3390/en14071800>

23. Zawadzki, M. et al. (2010). Effect of synthesis method of LSCF perovskite on its catalytic properties for phenol methylation. *Solid State Ion.*, 181(23–24), 1131–1139. <https://doi.org/10.1016/j.ssi.2010.06.009>.
24. Rao Somalu, M. (2016). Preparation of lanthanum strontium cobalt oxide powder by a modified sol-gel method. *Malaysian J. Anal. Sci.*, 20(6), 1458–1466. <https://doi.org/10.17576/mjas-2016-2006-26>
25. Abdul Malik, L. et al. (2021). Effect of nickel oxide - Modified BaCe_{0.54}Zr_{0.36}Y_{0.10}Er_{0.95} as composite anode on the performance of proton-conducting solid oxide fuel cell. *Int. J. Hydrog. Energy*, 46(8), 5963–5974. <https://doi.org/10.1016/j.ijhydene.2020.10.219>
26. Haile, S. M. et al. (2001). Non-stoichiometry, grain boundary transport and chemical stability of proton conducting perovskites. *J. Mater. Sci.*, 36(5), 1149–1160. <https://doi.org/10.1023/A:1004877708871>
27. Zhao, P. et al. (2018). Error analysis and correction for quantitative phase analysis based on rietveld-internal standard method: Whether the minor phases can be ignored? *Crystals*, 8(3), 110–113. <https://doi.org/10.3390/cryst8030110>
28. Zhao, S. et al. (2020). Performance of Ba_{0.5}Sr_{0.5}Co_{0.8}Fe_{0.2}O_{3-δ}/Ce_{0.85}Sm_{0.15}O_{2-δ}-CuO as a cathode for intermediate temperature solid oxide fuel cells. *J. Alloys Compd.*, 825, 154013. <https://doi.org/10.1016/j.jallcom.2020.154013>
29. Wang, H. et al. (2019). Enhancing catalysis activity of La_{0.6}Sr_{0.4}Co_{0.8}Fe_{0.2}O_{3-δ} cathode for solid oxide fuel cell by a facile and efficient impregnation process. *Int. J. Hydro. Energy*, 44(26), 13757–13767. <https://doi.org/10.1016/j.ijhydene.2019.03.184>
30. Xi, X. et al. (2016). LSCF–GDC composite particles for solid oxide fuel cells cathodes prepared by facile mechanical method. *Adv. Powder Techno.*, 27(2), 646–651. <https://doi.org/10.1016/j.apt.2016.02.022>
31. Siregar, N. et al. (2021). Effect of postheating temperature on efficiency of dye-sensitized solar cell with ZnO:Al thin films prepared by sol-gel spin coating. *J. Phys. Sci.*, 32(2), 57–70. <https://doi.org/10.21315/jps2021.32.2.5>
32. Muhammed Ali, S. A. et al. (2018). Influence of oxygen ion enrichment on optical, mechanical, and electrical properties of LSCF perovskite nanocomposite. *Ceram. Int.*, 44(9), 10433–10442. <https://doi.org/10.1016/j.ceramint.2018.03.060>
33. Ku, Y. et al. (2018). Chemical looping with air separation (CLAS) in a moving bed reactor with CuO/ZrO₂ oxygen carriers. *Int. J. Greenhouse Gas Cont.*, 70, 225–235. <https://doi.org/10.1016/j.ijggc.2017.12.009>.
34. Muhammed Ali, S. A. et al. (2018). Optical, mechanical and electrical properties of LSCF–SDC composite cathode prepared by sol–gel assisted rotary evaporation technique. *J. Sol-Gel Sci. Tech.*, 86(2), 493–504. <https://doi.org/10.1007/s10971-018-4636-8>
35. Flura, A. et al. (2016). Application of the Adler-Lane-Steele model to porous La₂NiO_{4+δ} SOFC cathode: Influence of interfaces with gadolinia doped ceria. *J. Electrochem. Society*, 163(6), 523–532. <https://doi.org/10.1149/2.0891606jes>

36. Giuliano, A. et al. (2017). Characterisation of $\text{La}_{0.6}\text{Sr}_{0.4}\text{Co}_{0.2}\text{Fe}_{0.8}\text{O}_{3-\delta}$ – $\text{Ba}_{0.5}\text{Sr}_{0.5}\text{Co}_{0.8}\text{Fe}_{0.2}\text{O}_{3-\delta}$ composite as cathode for solid oxide fuel cells. *Electrochim. Acta*, 240, 258–266. <https://doi.org/10.1016/j.electacta.2017.04.079>
37. Sharma, R. K. et al. (2019). Highly efficient architected Pr6O11 oxygen electrode for solid oxide fuel cell. *J. Power Sources*, 419, 171–180. <https://doi.org/10.1016/j.jpowsour.2019.02.077>
38. Irshad, M. et al. (2022). Influence of sintering temperature on the structural, morphological, and electrochemical properties of NiO-YSZ anode synthesized by the autocombustion route. *Metals*, 12(2), 219. <https://doi.org/10.3390/met12020219>